Electrical behavior of a graphene/PEKK and carbon black/PEKK nanocomposites in the vicinity of the percolation threshold

Camille Bessaguet, Eric Dantras, Guilhem Michon, Mathieu Chevalier, Lydia Laffont, Colette Lacabanne

Electrical behavior of a graphene/PEKK and carbon black/PEKK nanocomposites in the vicinity of the percolation threshold

C. Bessaguet[a,b,c], E. Dantras[b,*], G. Michon[c], M. Chevalier[a], L. Laffont[d], C. Lacabanne[b]

[a] Institut de Recherche Technologique (IRT) Saint Exupéry, 118 route de Narbonne, CS 44248, 31432 Toulouse, Cedex 4, France
[b] CIRIMAT, Université de Toulouse, CNRS, UPS, Physique des Polymères, 118 route de Narbonne, 31062 Toulouse, Cedex 09, France
[c] Institut Supérieur de l'Aéronautique et de l'espace, Institut Clément Ader, 3 rue Caroline Aigle, 31400 Toulouse, France
[d] CIRIMAT, Université de Toulouse, CNRS, INPT, ENSIACET, 4 allée Emile Monso, CS44362, 31030 Toulouse, France

ARTICLE INFO

Keywords:
Conductive nanocomposite
Poly(ether ketone ketone)
Graphene
Carbon black
Percolation threshold
Electrical conductivity
Dielectric permittivity
Mechanical moduli

ABSTRACT

Graphene and carbon black have been dispersed in a high performance thermoplastic polymer, the poly(ether ketone ketone), to improve its electrical conductivity. The dispersion of graphene has a significant influence on the percolation threshold. A simple exfoliation protocol to obtain graphene monolayers has led to a significant decrease of the percolation threshold from 4.2 to 1.9 vol%. To the best of our knowledge, it is one of the lowest percolation values for unfunctionalized graphene dispersed by melt blending in a high performance thermoplastic matrix. The conductivity value above the percolation threshold (1.2 $S{\cdot}m^{-1}$) means that graphene was not degraded during the elaboration process. Below the percolation threshold, Maxwell-Wagner-Sillars phenomenon increases the dielectric permittivity from 2.7 to 210 for PEKK/6 vol% graphene at 180 °C and 1 Hz. Dynamic mechanical analyses have shown that mechanical moduli were not significantly modified by conductive particles until 6 vol%.

1. Introduction

High performance thermoplastic composites raise a growing interest for structural applications in aeronautical and space industries. In order to improve their electrical properties, the introduction of conductive particles (metal or carbon) within the polymer matrix has been the subject of many studies. Usually, metallic fillers like gold [1,2] or silver fillers [3–5] permit to reach high electrical conductivity (σ = 10^2–10^3 $S{\cdot}m^{-1}$) but their high density implies an increase of the structure weight. Due to their low density, carbon fillers as carbon black [6], carbon nanotubes [7,8] or graphene [9] are of interest in a wide range of applications, where a high electrical conductivity for electrical dissipation (σ = 0.1–1 $S{\cdot}m^{-1}$) is not required [10]. In order to maintain the mechanical properties of the matrix, for low particle content, conduction phenomenon may occur. The critical transition from an insulating to a conducting behavior is associated with the percolation threshold. It corresponds to the formation of an infinite conducting path within the material. The value of the percolation threshold only depends on the apparent conductive particle aspect ratio ξ [11,12]. Lower percolation thresholds are reached for particles with a high aspect ratio. For example, percolation threshold is observed near 8–10 vol% [13] with carbon black ($\xi \approx 1$) and lower than 0.4 vol% [14] with carbon nanotubes ($\xi \approx$ 1000–10,000).

In the present work, graphene was used for the elaboration of conductive nanocomposites. Graphene was recently highlighted by Novoselov and Geim in 2004 [15,16]. Its good electrical properties and high aspect ratio have aroused great interest among the scientific community [17–21]: high charge mobility (230,000 cm^2/Vs), low visible light absorption (2.3%), high thermal conductivity (3000 W/mK), high strength (130 GPa), high elastic modulus (1 TPa) and the highest theoretical specific surface area (2600 m^2/g). A reference sample processed with spherical carbon black was also elaborated to compare with graphene.

The poly(ether ketone ketone) (PEKK) was used as polymer matrix. It is a high performance thermoplastic polymer that belongs to the poly(aryl ether ketone) family. One of the main advantages of PEKK is that the melting point can be modulated, as reported by Gardner [22]. 100% para PEKK and para - iso PEKK show differences in the melting point temperature, whereas the glass transition temperature stays quasi constant. By increasing the proportion of meta isomers, defects in the crystal packing decrease the melting point temperature and enhance the processing conditions.

The processing of nanocomposite and, more specifically, the dispersion of particle is the most important challenge to obtain

* Corresponding author.
E-mail address: eric.dantras@univ-tlse3.fr (E. Dantras).

https://doi.org/10.1016/j.jnoncrysol.2019.02.017

macroscopic homogeneous properties. Due to strong interactions between graphene sheets, it makes difficult to disperse them randomly in the polymer matrix. Especially in case of graphene, aggregates could be generated and decrease the apparent aspect ratio [17,23,24]. In order to improve the graphene dispersion in nanocomposites several exfoliation ways are studied. The solvent way, which uses commonly *N*-methyl-2-pyrrolidone [25] or *N*,*N*-dimethylformamide [26], is an easy process that can bring high graphene concentration (higher than 1 mg·mL^{-1}) but leads to use solvent. An aqueous way have been proposed with an anionic surfactant as sodium dodecyl sulfate for example. In this case, high graphene concentration is more difficult to obtain [27–29].

The manuscript presents the protocol to graphene exfoliation and the processing used for PEKK/graphene and PEKK/carbon black nanocomposites. The influence of the nature of conductive fillers on dielectric properties such as electrical conductivity and dielectric permittivity and mechanical properties such as storage and loss moduli were studied.

2. Experimental section

2.1. Materials

Poly(ether ketone ketone) PEKK (Arkema) (diameter of powder 20 µm) and Carbon black (CB, glassy carbon from Sigma Aldrich), were supplied in powder, respectively. Graphene (GR from Avanzare) was supplied in ethanol suspension (EtOH) with a concentration of 0.5 wt%. The morphology of GR and CB was investigated by scanning electron microscopy (SEM - FEG JEOL JSM 7800F Prime) using secondary electron detector. Fig. 1 shows the SEM images of CB (a) and "as received" GR (b), respectively.

The CB particles are spherical with a mean diameter of 6.3 µm (d_{50}) determined using a laser granulometer (Fig. 1a). Fig. 1b shows graphene stack due to the SEM resolution, which does not allow to observe GR monolayers. To analyze precisely the GR nanotexture, images were performed using a JEOL JEM 2100F electron microscope operated at 200 kV. Diffraction patterns were recorded using selected area electron diffraction (SAED) mode with a 150nm aperture.

Fig. 2 is a bright field image of GR and one monolayer is visible in the black circle, which indicates the selected area for the SAED pattern. This pattern is characteristic of one graphene layer (P63/mmc, a = 2461 Å and c = 6708 Å). The wrinkled aspect and the grey contrast differences suggest that GR is also composed by a large amount of GR multilayers classically labelled exfoliated graphene nanoplatelets in the literature [30]. This local microscopic observation is not appropriate to characterize the entire GR batch. The number of GR layers modifies the apparent aspect ratio and has a significant influence on nanocomposite electrical properties. The electrical percolation threshold allows us to determine the apparent aspect ratio of these particles.

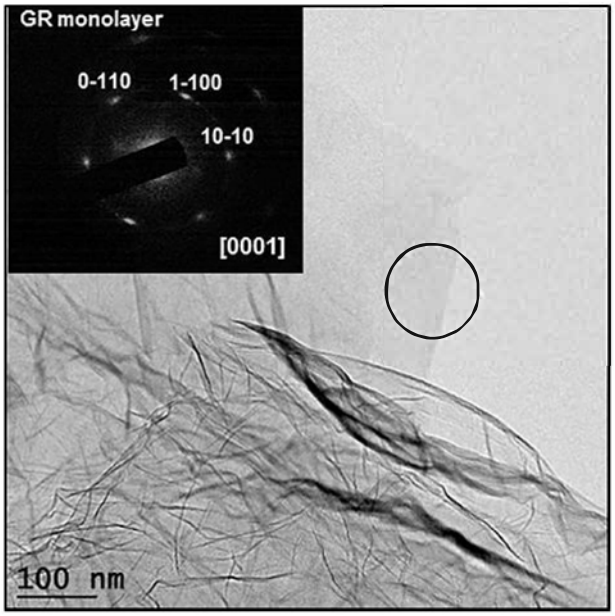

Fig. 2. Bright field TEM image of the "as received" graphene. The black circle shows the area selected for the SAED pattern (in insert).

2.2. Nanocomposite processing

In order to manage the distribution of GR in the polymer, a simple protocol was applied. It consists in two steps process: a GR exfoliation followed by a decantation. For exfoliation an aqueous solution with sodium dodecyl sulfate (SDS) as surfactant was chosen [29]. SDS was solubilized in EtOH at 2.4 mg·mL^{-1}. It corresponds to the critical micellar concentration (CMC) in water. GR suspension was diluted in a solution containing EtOH and SDS following the 3/5 ratio, respectively. Suspension was sonicated for 1 min (power 300 W). After 10 min of decantation, GR suspension was collected to process the nanocomposite.

For the PEKK/GR (GR-NC) and PEKK/CB (CB-NC) nanocomposites processing, a premix powder was used. GR/EtOH or CB/EtOH suspensions and polymer powder (20 µm in diameter) were mixed.

PEKK polymer powder is in suspension in this mix. Then it was sonicated with ultrasound to promote a homogeneous dispersion. EtOH

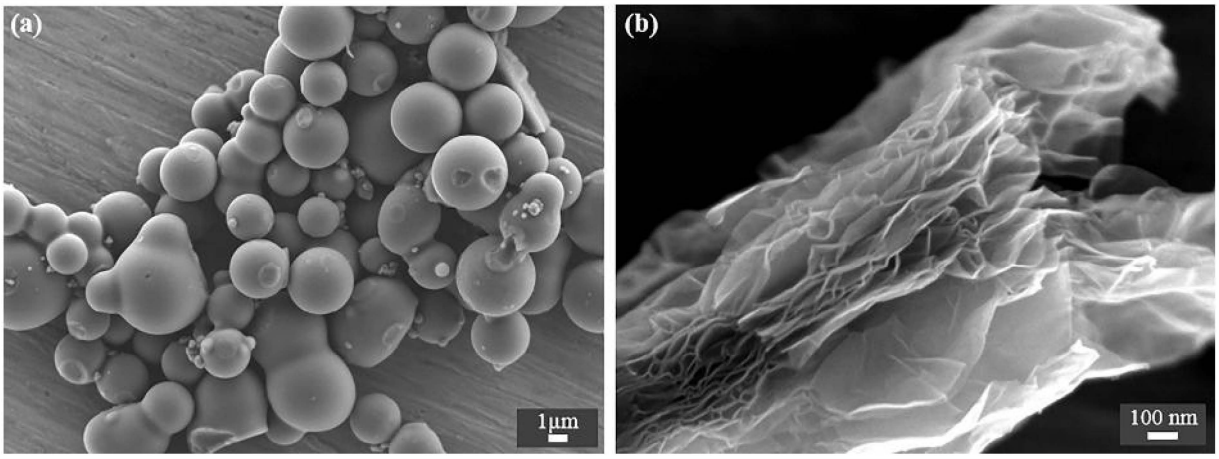

Fig. 1. SEM images of carbon black (a) and the "as received" graphene (b).

was evaporated with a rotary evaporator at 80 °C. Nanocomposites were elaborated through melt blending at 360 °C with mechanical mixing using a laboratory twin screw extruder (GR-NC1). GR-NC2, GR-NC3 and CB-NC were processed with hot press. GR-NC1 was elaborated from "as received" GR without any treatment. GR-NC2 was elaborated from GR exfoliated according to the previously described protocol. GR-NC3 was elaborated from GR exfoliated by the commercial supplier. As it has been reported in previous works, this protocol leads to a very good particle dispersion in polymer matrix even for high aspect ratio [1,4,5,14]. The nanocomposite electrical conductivity study, and more specifically, the percolation threshold value allows us to analyze the dispersion quality at a macroscopic scale. As the percolation threshold theoretical value of spherical particles dispersion is well known, CB-NC was elaborated to check the dispersion protocol.

2.3. Dielectric and mechanical analyses

Dynamic electrical conductivity and dielectric permittivity of nanocomposites were performed from −150°C to 200 °C and 10^{-2} Hz to 10^{6} Hz using a Novocontrol Broadband Dielectric Spectrometer (BDS). Disk-shape samples (20 mm in diameter) have been processed by compression molding at 360 °C to determine the bulk electrical conductivity. In order to promote a 3D conductivity, thick samples were hot pressed (1 mm thickness).

To extract the percolation threshold value the following Eq. (1) was used [31,32]:

$$\sigma_{DC} = \sigma_0 (p - p_c)^t \quad (1)$$

where σ_{DC} is the static nanocomposite conductivity, σ_0 the GR pathway conductivity, p the GR content, p_c the percolation threshold and t the universal critical exponent that depends on the system dimensionality ($1 < t < 1.3$ for a 2D network and $1.5 < t < 2$ for a 3D network [31,32]).

Dynamic mechanical analyses (DMA) were carried out on PEKK, GR-NC1 and CB-NC using an ARES G1 TA Instruments apparatus in shear mode, from −130 °C to 270 °C at 3 °C·min^{-1}. The applied strain and frequency were fixed at 0.1% and 0.16 Hz (an angular frequency of 1 rad·s^{-1}), respectively. Parallelepipedic samples with 40 mm long, 10 mm wide and 0.6 mm thick were studied.

3. Results & discussion

3.1. Study of the dispersion quality by bulk electrical conductivity analysis

Fig. 3 represents the DC conductivity behavior at room temperature as a function of GR and CB content: GR-NC1 (PEKK/"as received" GR nanocomposites), GR-NC2 (PEKK/lab-exfoliated GR nanocomposites), GR-NC3 (PEKK/supplier exfoliated GR nanocomposites) and CB-NC (PEKK/CB nanocomposites).

For GR-NC1 the percolation threshold is determined near 4.2 vol%, the conductivity value above p_c reaches 4.9×10^{-4} S·m^{-1}. The percolation threshold decreases until 3 vol% after the exfoliation/decantation protocol (GR-NC2) and the conductivity value above p_c is 6.5×10^{-2}S·m^{-1}. For GR-NC3, the percolation threshold is even lower (1.9 vol%) with the highest conductivity value of 1.2 S·m^{-1}.

In order to compare these results with a reference material, CB nanocomposites were elaborated. The percolation threshold for CB-NC is determined at 16.2 vol%.

The percolation threshold value is highly dependent on the GR dispersion, which is associated with the elaboration process, the GR aspect ratio and its surface modification. Kim et al. [33] have shown the influence of elaboration process by comparing three technics: in solution, in-situ polymerization and melt process. The first and second one lead to the lowest percolation threshold due to the very low viscosity of the mixture [34]. For example, Stankovich et al. [23] dispersed GR (chemically modified) in polystyrene (PS) and they reached a

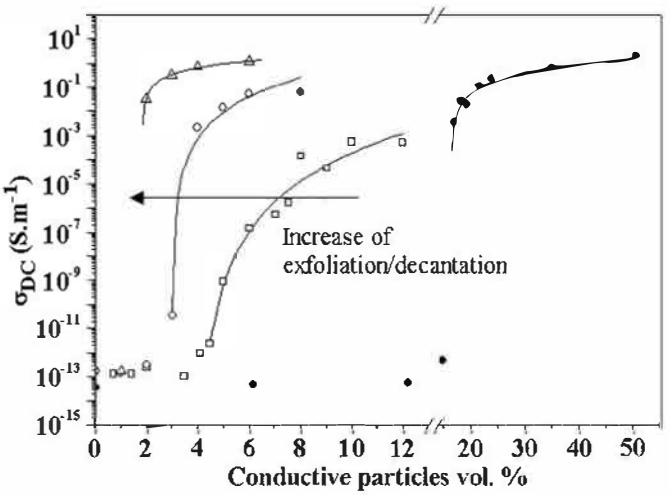

Fig. 3. DC conductivity versus conductive particles volume fraction for GR-NC1 (□), GR-NC2 (○), GR-NC3 (△) and CB-NC (●). Solid line is the percolation threshold fit.

percolation threshold near 0.1 vol%. The GR dispersion in the viscous polymer melt is more difficult. The GR functionalization is used to generate repulsive interactions between layers. Yang et al. in 2013 [35] dispersed GR functionalized poly(ethersulfone) (PES) in PEEK. They obtained a percolation threshold of 0.76 vol%. However, the GR sheets functionalization leads to structural defects and the GR electrical conductivity decreases. Thus, conductivity values above the percolation threshold are generally lower in the case of functionalized GR [23,35] in comparison with unfunctionalized ones [12,24,36].

GR aggregates decrease the apparent aspect ratio and increase the percolation threshold. This work was consistent with those carried out by Tkalya [12], which works on the dispersion of unfunctionalized GR in a poly(styrene) matrix. Their percolation thresholds values (between 2 and 4.5 vol%) or conductivities (between 1 and 10 S·m^{-1}) results were similar to PEKK/GR nanocomposite.

The percolation threshold for CB-NC determined at 16.2 vol% is closed to the theoretical value [37]; i.e. perfect sphere randomly dispersed. It is important to note that many factors could affect this experimental percolation threshold value [38].

Fig. 4 reports the linear fit of $log(\sigma_{DC})$ as a function of $(p - p_c)$. Extracted values of p_c, σ_0 and t were reported in the Table 1 for GR-NC1, GR-NC2, GR-NC3 and CB-NC.

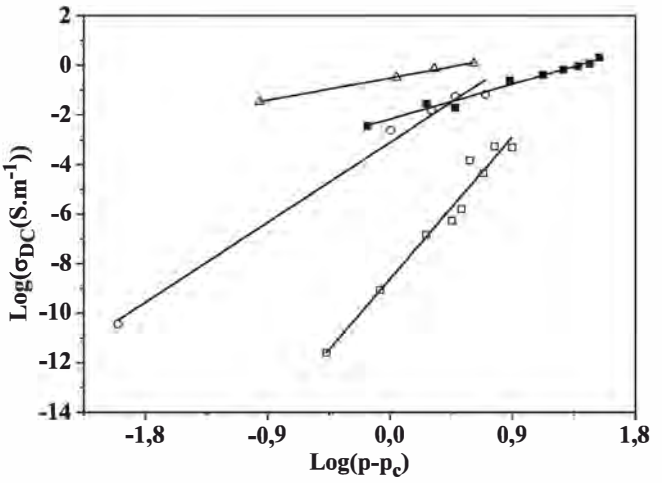

Fig. 4. Power law fit for GR-NC1 (□), GR-NC2(○), GR-NC3 (△) and CB-NC (●). Solid line is the linear fit.

Table 1
Processing methods and percolation law parameters.

	Processing	p_c (vol%)	σ_0 (S·m^{-1})	t
GR-NC1	Extrusion	4.2	2.5×10^{-9}	6.4
GR-NC2	Hot press	3.0	7.9×10^{-4}	3.6
GR-NC3	Hot press	1.9	3.1×10^{-1}	1.0
CB-NC	Hot press	16.2	6.3×10^{-3}	1.6

Universal critical exponent values of GR-NC1 and GR-NC2 were 6.4 and 3.6, respectively. These values are higher than the estimated values ($1.5 < t < 2$ for a 3D network [31,32]). In the literature, high t values have already been identified in GR/polymer nanocomposites: 5.8 for PEEK/GR nanocomposites [35], 3.8 for PVDF/GR nanocomposites [39], 3.2 for ABS/GR and SAN/GR nanocomposites [40]. Authors attributed this behavior to the inhomogeneity of the GR dispersion. Aggregates or folding limited the electronic transport within the nanocomposite and increased the t value. Thus, it is consistent with GR-NC3 results; i.e. a better dispersion leads to a decrease of t at 1.

GR-NC1 nanocomposites, elaborated by extrusion from a premix nanocomposite powder, has a very low conductivity above the percolation threshold (10^{-3} S·m^{-1}). The shear and compression strengths during the extrusion process alter the electrical properties. These observations, already reported in the literature, were related to the reduction of exfoliated graphene nanoplatelets aspect ratio [41] and/or re-agglomeration phenomenon [42]. The conductivity above the percolation threshold is thereby greatly reduced. σ_0 is related to the intrinsic conductivity of the pristine GR sheet [26] (generally known at 10^3 S·m^{-1} for carbon particles).

The GR-NC3 nanocomposite has the higher σ_0. This elaboration protocol (exfoliation/decantation then hot press lamination) promote better GR electrical properties. Finally, as regards CB-NC nanocomposites, the CB intrinsic conductivity σ_0 is 6.3×10^{-3} S·m^{-1}. It is an intermediate value between GR-NC2 and GR-NC3; t value is 1.6, which corresponds to a 3D network [31,32]. For GR-NC (1.2 S·m^{-1} at 6 vol%) and CB-NC (1.0 S·m^{-1} at 50vol%), we noticed that the maximum of conductivity above the percolation threshold was similar in both cases. This value was clearly dependent from the particle nature (carbonaceous as comparison with metallic particles).

3.2. Influence of graphene on the conductivity frequency and temperature dependence

Fig. 5 represents the evolution of the real part of the electrical conductivity as a function of frequency from −150°C to 200 °C. Experiments were carried out for PEKK/home-exfoliated GR (GR-NC2) with 3 and 4 vol%; i.e. in the vicinity of the percolation threshold. Two behaviors are highlighted as a function of frequency: below p_c, conductivity is dependent on frequency. This behavior is consistent with the Jonscher universal power law for an insulator [43]. Above p_c, conductivity is not dependent on frequency: it is associated with a conductor behavior.

In both cases conductivity increased with temperature for a wide range of frequency. The real part of the complex conductivity is composed of two terms: a direct courant conductivity σ_{DC} and an alternating courant conductivity σ_{AC} which is frequency dependent (Eq. (2)).

$$\sigma'(\omega) = \sigma_{DC} + \sigma_{AC}(\omega) \quad (2)$$

For a critical frequency ω_c, a change of the electronic conduction phenomenon occurred:

$$\text{For } \omega < \omega_c \quad \sigma'(\omega) = \sigma_{DC} \quad (3)$$

$$\text{For } \omega > \omega_c \quad \sigma'(\omega) = \sigma_{AC}(\omega) = A\omega^s \quad (4)$$

where A is a pre-exponential constant and s, the power law exponent ($0 < s < 1$). The inset graph in Fig. 5 represents the evolution of the s exponent as a function of temperature for PEKK/3 vol% GR-NC2 (below p_c). The exponent s was calculated by fitting the experimental data with a power law for each isotherm. Two behaviors were identified. Below −50C, the s temperature dependence is weak. It means that two electronic conduction behaviors exist in the vicinity of the percolation threshold: tunneling effect below −50°C and hopping activation process above. At low temperature, tunneling effect is not temperature dependent whereas hopping is thermally activated. In both case, electronic transport through the conductive path do not require a surface contact between GR or CB particles.

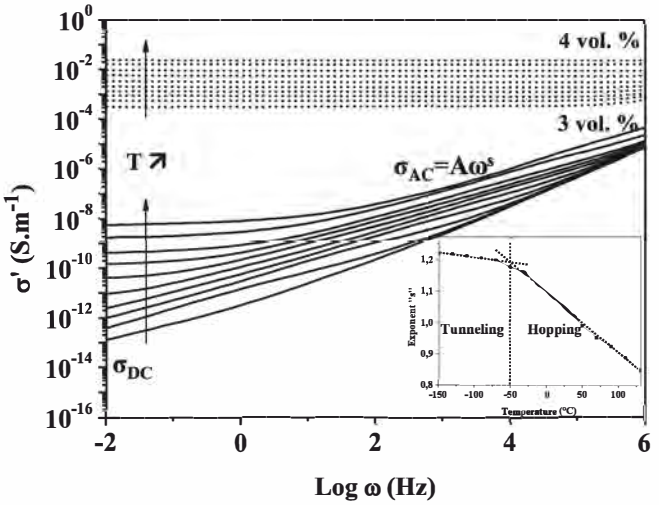

Fig. 5. Real part of the conductivity versus frequency for PEKK/home-exfoliated graphene (GR-NC2) 3 vol% (solid line) and 4 vol% (dashed line) for isotherms from −150°C to 200 °C.

3.3. Influence of graphene on the dielectric permittivity in the vicinity of the percolation threshold

Dielectric permittivity has been studied for GR-NC1 nanocomposites in order to analyze behaviors within the gradual percolation threshold. Fig. 6(a) presents the evolution of permittivity measured at 1 Hz as a function of GR content for different temperatures: at room temperature, near the glass transition temperature and above 20 °C, 160 °C and 180 °C, respectively. The inset graph in Fig. 6(a) represents the DC conductivity as a function of GR content, each composite relative to the percolation threshold is identified (★).

The introduction of graphene leads to an increase of the dielectric permittivity in the vicinity of the percolation threshold. Permittivity increases from 2.7 for the neat PEKK to 83 for PEKK/6 vol% GR at room temperature (the dielectric permittivity value reaches 210 at 180 °C).

Classically, the real part of the dielectric permittivity increases above the dielectric manifestation of the glass transition temperature. But at low frequency, an additional dielectric phenomenon can be observed. Fig. 6(b) represents the evolution of the real part of the permittivity measured at room temperature as a function of frequency for different graphene contents. At low frequency, permittivity increases with the graphene fraction. For GR-NC1 with 6 vol%, permittivity increases from 20 at 100 kHz to 83 at 1 Hz. It has been already shown that the introduction of conductive particles into a dielectric polymer matrix increases the dielectric permittivity [39,44,45]. It has been associated with a Maxwell – Wagner - Sillars (MWS) polarization: electric charges are trapped at the particle/matrix interface [46,47]. This dielectric phenomenon could have a specific interest for electronic devices [6].

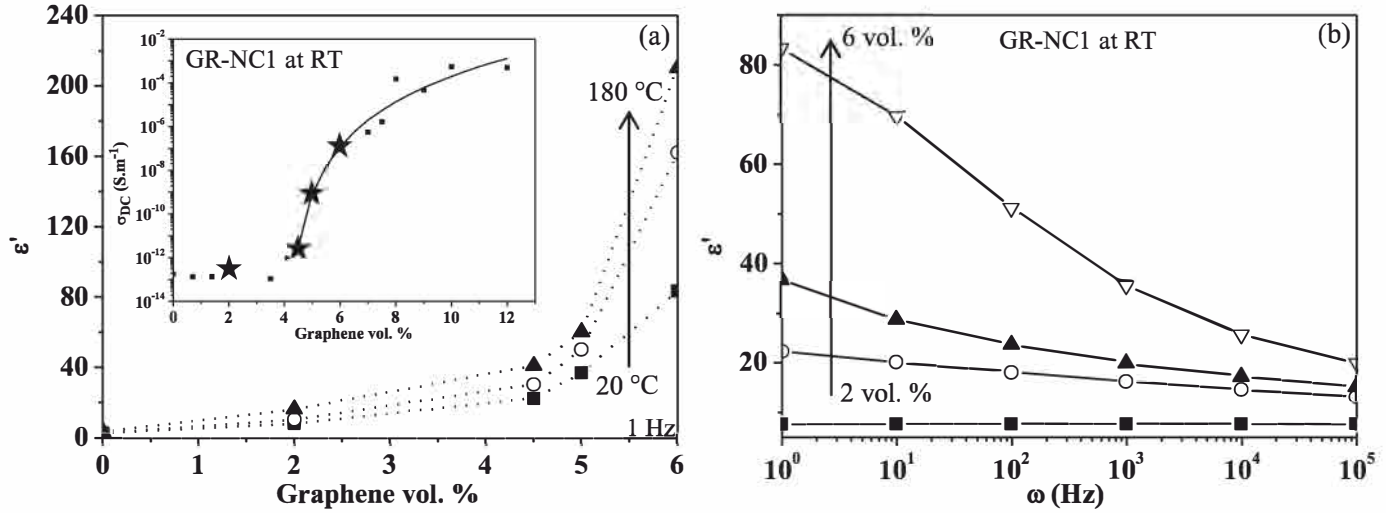

Fig. 6. (a) Real part of the dielectric permittivity versus graphene vol% for PEKK and PEKK/"as received" graphene (GR-NC1) at (■) 20 °C, (○) 160 °C and (▲) 180 °C. Inset: DC conductivity versus GR content at room temperature. (b) Real part of the dielectric permittivity versus frequency for PEKK and PEKK/"as received" graphene (GR-NC1) at room temperature: (■) 2 vol% graphene, (○) 4.5 vol% graphene, (▲) 5 vol% graphene and (▽) 6 vol% graphene. Solid lines are guide for the eye.

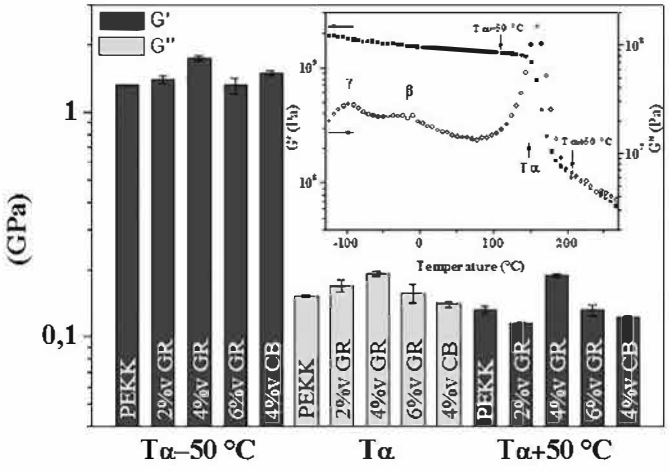

Fig. 7. Storage modulus G' and loss modulus G" of unfilled PEKK, PEKK/2 vol% GR, PEKK/4 vol% GR, PEKK/6 vol% GR and PEKK/4 vol% CB, measured at Tα − 50°C, Tα and Tα + 50°C. Inset: PEKK matrix thermogram between −130 °C and 270 °C.

3.4. Influence of graphene on the mechanical properties below the percolation threshold

The improvement of electrical properties of high performance thermoplastic should be done without altering their mechanical properties. The influence of carbon particles (GR-NC1 or CB-NC) on the conservative and dissipative moduli has been determined in comparison with unfilled PEKK. G' and G'' values were determined at $T_\alpha - 50^\circ C$ (vitreous plateau), T_α (in the viscoelastic relaxation domain) and $T_\alpha + 50^\circ C$ (rubbery plateau) and reported in Fig. 7. The inset graph in Fig. 7 shows the PEKK thermogram over all the temperature range. The study of the mechanical relaxations have been extensively detailed in a previous paper [48].

Mechanical properties of PEKK and its composites are presented in Fig. 7. Considering the error bars, the particles until 6 vol% do not influence significantly the mechanical moduli even for graphene. Thus, the high performance mechanical properties of the polymer matrix is maintained.

4. Conclusion

Commercial graphene and carbon black were satisfactory dispersed in a high performance thermostable thermoplastic PEKK polymer in order to improve their electrical properties. Particle aspect ratio has a strong influence on the percolation threshold value. It decreased from 16.2 vol% with carbon black ($\xi \approx 1$) to 4.2 vol% with an "as received" graphene (GR-NC1) and 1.9 vol% after a graphene exfoliation/decantation process (GR-NC3). Exfoliation/decantation improved the graphene dispersion by limiting the number of layer and increasing the graphene aspect ratio. Above the percolation threshold, high conductivity values (1–1.2 $S{\cdot}m^{-1}$) were obtained for graphene and carbon black. It was one decade higher than the conductivity measured for carbon nanotubes nanocomposites. Graphene pathway also increased dielectric permittivity from 2.6 for PEKK to 83 for the PEKK/6 vol% GR nanocomposite. Finally, until 6 vol% graphene and 4 vol% carbon black, nanocomposite mechanical behaviors are not significantly modified.

Acknowledgments

These results were obtained under the research project "COMPINNOVTP" at the IRT Saint Exupéry. We thank the industrial and academic members of the IRT who supported this project through their contributions, both financial and in terms of specific knowledge: AIRBUS OPERATIONS, ARIANE GROUP, AIRBUS HELICOPTERS, AIRBUS GROUP INNOVATIONS, THALES ALENIA SPACE, CIRIMAT, ISAE, ICA, IMRCP, UPS and CNRS. We also thank the Commissariat Général aux Investissements and the Agence Nationale de la Recherche for their financial support in the Programme d'Investissement d'Avenir (PIA).

References

[1] L. Ramachandran, A. Lonjon, P. Demont, E. Dantras, C. Lacabanne, Conduction mechanisms in P(VDF-TrFE)/gold nanowire composites: tunnelling and thermally-activated hopping process near the percolation threshold, Mater. Res. Express. 3 (2016) 085027.

[2] M.C. Salvadori, F.S. Teixeira, L.G. Sgubin, M. Cattani, I.G. Brown, Electrical conductivity of gold-implanted alumina nanocomposite, Nucl. Instruments Methods Phys. Res. Sect. B Beam Interact. Mater. Atoms 310 (2013) 32–36, https://doi.org/10.1016/j.nimb.2013.05.024.

[3] W. Zheng, X.F. Lu, W. Wang, Z.J. Wang, M.X. Song, Y. Wang, C. Wang, Fabrication of novel Ag nanowires/poly(vinylidene fluoride) nanocomposite film with high

dielectric constant, Phys. Status Solidi A. 207 (2010) 1870–1873, https://doi.org/10.1002/pssa.200925520.
[4] L. Rivière, A. Lonjon, E. Dantras, C. Lacabanne, P. Olivier, N.R. Gleizes, Silver fillers aspect ratio influence on electrical and thermal conductivity in PEEK/Ag nanocomposites, Eur. Polym. J. 85 (2016) 115–125, https://doi.org/10.1016/j.eurpolymj.2016.08.003.
[5] L.Q. Cortes, A. Lonjon, E. Dantras, C. Lacabanne, High-performance thermoplastic composites poly(ether ketone ketone)/silver nanowires: morphological, mechanical and electrical properties, J. Non-Cryst. Solids 391 (2014) 106–111, https://doi.org/10.1016/j.jnoncrysol.2014.03.016.
[6] J.X.J. Xu, M. Wong, C.P. Wong, Super high dielectric constant carbon black-filled polymer composites as integral capacitor dielectrics, 2004 Electron, Components Technol. Conf. 1 (2004) 536–541, https://doi.org/10.1109/ECTC.2004.1319391.
[7] P. Van Durmen, Etude de l'influence de la dispersion de nanotubes de carbone sur les propriétés électriques de composites à matrice PEEK, Thèse Université de Toulouse, 2014.
[8] D. Carponcin, E. Dantras, J. Dandurand, G. Aridon, F. Levallois, L. Cadiergues, C. Lacabanne, Discontinuity of physical properties of carbon nanotube/polymer composites at the percolation threshold, J. Non-Cryst. Solids 392–393 (2014) 19–25, https://doi.org/10.1016/j.jnoncrysol.2014.03.022.
[9] V. Dhand, K.Y. Rhee, H.J. Kim, D.H. Jung, A comprehensive review of graphene nanocomposites: research status and trends, J. Nanomater. 14 (2013) 1–50.
[10] R. Sanjinés, M.D. Abad, C. Vâju, R. Smajda, M. Mionić, A. Magrez, Electrical properties and applications of carbon based nanocomposite materials: an overview, Surf. Coatings Technol. 206 (2011) 727–733, https://doi.org/10.1016/j.surfcoat.2011.01.025.
[11] T. Kuilla, S. Bhadra, D. Yao, N.H. Kim, S. Bose, J.H. Lee, Recent advances in graphene based polymer composites, Prog. Polym. Sci. 35 (2010) 1350–1375, https://doi.org/10.1016/j.progpolymsci.2010.07.005.
[12] E. Tkalya, M. Ghislandi, R. Otten, M. Lotya, A. Alekseev, P. Van Der Schoot, J. Coleman, G. De With, C. Koning, Experimental and theoretical study of the influence of the state of dispersion of graphene on the percolation threshold of conductive graphene/polystyrene nanocomposites, Appl. Mater. Interfaces 6 (2014) 15113–15121.
[13] A.I. Medalia, Electrical conduction in carbon black composites, Rubber Chem. Technol. 59 (1986) 432–454, https://doi.org/10.5254/1.3538209.
[14] D. Carponcin, E. Dantras, G. Aridon, F. Levallois, L. Cadiergues, C. Lacabanne, Evolution of dispersion of carbon nanotubes in polyamide 11 matrix composites as determined by DC conductivity, Compos. Sci. Technol. 72 (2012) 515–520.
[15] K.S. Novoselov, A.K. Geim, S.V. Morozov, D. Jiang, Y. Zhang, S.V. Dubonos, I.V. Grigorieva, A.A. Firsov, Electric field effect in atomically thin carbon films, Science (80-.) 306 (2004) 666–669.
[16] K.S. Novoselov, D. Jiang, F. Schedin, T.J. Booth, V.V. Khotkevich, S.V. Morozov, A.K. Geim, Two-dimensional atomic crystals, Proc. Natl. Acad. Sci. U. S. A 102 (2005) 10451–10453, https://doi.org/10.1073/pnas.0502848102.
[17] V. Singh, D. Joung, L. Zhai, S. Das, S.I. Khondaker, S. Seal, Graphene based materials: past, present and future, Prog. Mater. Sci. 56 (2011) 1178–1271, https://doi.org/10.1016/j.pmatsci.2011.03.003.
[18] K.I. Bolotin, K.J. Sikes, Z. Jiang, M. Klima, G. Fudenberg, J. Hone, P. Kim, H.L. Stormer, Ultrahigh electron mobility in suspended graphene, Solid State Commun. 146 (2008) 351–355, https://doi.org/10.1016/j.ssc.2008.02.024.
[19] R.R. Nair, P. Blake, A.N. Grigorenko, K.S. Novoselov, T.J. Booth, T. Stauber, N.M.R. Peres, A.K. Geim, Fine structure constant defines visual transperency of graphene, Science (80-.) 320 (2008) 1308, https://doi.org/10.1126/science.1156965.
[20] J.H. Seol, I. Jo, A.L. Moore, L. Lindsay, Z.H. Aitken, M.T. Pettes, X. Li, Z. Yao, R. Huang, D. Broido, N. Mingo, R.S. Ruoff, L. Shi, Two-dimensional phonon transport in supported graphene, Science. 328 (2010) 213–216, https://doi.org/10.1126/science.1184014.
[21] C. Lee, X. Wei, J.W. Kysar, J. Hone, Measurement of elastic properties and intrinsic strength of monolayer graphene, Science (80-.) 321 (2008) 385–388.
[22] K.H. Gardner, B.S. Hsiao, R.R. Matheson, B.A. Wood, Structure, crystallization and morphology of poly (aryl ether ketone ketone), Polymer (Guildf). 33 (1992) 2483–2495, https://doi.org/10.1016/0032-3861(92)91128-O.
[23] S. Stankovich, D.A. Dikin, G.H.B. Dommett, K.M. Kohlhaas, E.J. Zimney, E.A. Stach, R.D. Piner, S.T. Nguyen, R.S. Ruoff, Graphene-based composite materials, Nature. 442 (2006) 282–286, https://doi.org/10.1038/nature04969.
[24] Y.V. Syurik, M.G. Ghislandi, E.E. Tkalya, G. Paterson, D. McGrouther, O.A. Ageev, J. Loos, Graphene network organisation in conductive polymer composites, Macromol. Chem. Phys. 213 (2012) 1251–1258, https://doi.org/10.1002/macp.201200116.
[25] Y. Hernandez, V. Nicolosi, M. Lotya, F.M. Blighe, Z. Sun, S. De, I.T. Mcgovern, B. Holland, M. Byrne, Y.K.G.U.N. Ko, J.J. Boland, P. Niraj, G. Duesberg, S. Krishnamurthy, R. Goodhue, J. Hutchison, V. Scardaci, A.C. Ferrari, J.N. Coleman, High-yield production of graphene by liquid-phase exfoliation of graphite, Nat. Nanotechnol. 3 (2008) 563–568, https://doi.org/10.1038/nnano.2008.215.
[26] X. Li, H. Deng, Z. Li, H. Xiu, X. Qi, Q. Zhang, K. Wang, F. Chen, Q. Fu, Graphene/thermoplastic polyurethane nanocomposites: surface modification of graphene through oxidation, polyvinyl pyrrolidone coating and reduction, Compos. Part A 68 (2015) 264–275, https://doi.org/10.1016/j.compositesa.2014.10.016.
[27] P. Yang, F. Liu, Understanding graphene production by ionic surfactant exfoliation : a molecular dynamics simulation study, J. Appl. Phys. 116 (2014) 1–7, https://doi.org/10.1063/1.4885159.
[28] S. Wang, M. Yi, Z. Shen, X. Zhang, Adding ethanol can effectively enhance the graphene concentration in water – surfactant, R. Soc. Chem. 4 (2014) 25374–25378, https://doi.org/10.1039/c4ra03345k.
[29] C. Yeon, K. Lee, J.W. Lim, High-yield graphene exfoliation using sodium dodecyl sulfate accompanied by alcohols as surface-tension-reducing agents in aqueous solution, Carbon N. Y. 83 (2015) 136–143, https://doi.org/10.1016/j.carbon.2014.11.035.
[30] M.D. Via, J.A. King, J.M. Keith, G.R. Bogucki, Electrical conductivity modeling of carbon black/polycarbonate, carbon nanotube/polycarbonate, and exfoliated graphite nanoplatelet/polycarbonate composites, J. Appl. Polym. Sci. 124 (2012) 182–189, https://doi.org/10.1002/app.35096.
[31] S. Kirkpatrick, Percolation and conduction, Rev. Mod. Phys. 45 (1973) 574–588.
[32] D. Stauffer, A. Aharony, Introduction to Percolation Theory, 2nd Revised edition, Taylor & Francis, 1985.
[33] H. Kim, Y. Miura, C.W. Macosko, Graphene/polyurethane nanocomposites for improved gas barrier and electrical conductivity, Chem. Mater. 22 (2010) 3441–3450, https://doi.org/10.1021/cm100477v.
[34] K.H. Liao, Y. Qian, C.W. MacOsko, Ultralow percolation graphene/polyurethane acrylate nanocomposites, Polymer (Guildf). 53 (2012) 3756–3761, https://doi.org/10.1016/j.polymer.2012.06.020.
[35] L. Yang, S. Zhang, Z. Chen, Y. Guo, J. Luan, Z. Geng, G. Wang, Design and preparation of graphene/poly(ether ether ketone) composites with excellent electrical conductivity, J. Mater. Sci. 49 (2013) 2372–2382, https://doi.org/10.1007/s10853-013-7940-2.
[36] T. Kuila, S. Bose, P. Khanra, N.H. Kim, K.Y. Rhee, J.H. Lee, Characterization and properties of in situ emulsion polymerized poly(methyl methacrylate)/graphene nanocomposites, Compos. Part A 42 (2011) 1856–1861, https://doi.org/10.1016/j.compositesa.2011.08.014.
[37] H. Scher, R. Zallen, Critical density in percolation processes, J. Chem. Phys. 53 (1970) 3759–3761.
[38] W. Zhang, A.A. Dehghani-Sanij, R.S. Blackburn, Carbon based conductive polymer composites, J. Mater. Sci. 42 (2007) 3408–3418, https://doi.org/10.1007/s10853-007-1688-5.
[39] P. Fan, L. Wang, J. Yang, F. Chen, M. Zhong, Graphene/poly(vinylidene fluoride) composites with high dielectric constant and low percolation threshold, Nanotechnology 23 (2012) 1–8, https://doi.org/10.1088/0957-4484/23/36/365702.
[40] C. Gao, S. Zhang, F. Wang, B. Wen, C. Han, Y. Ding, M. Yang, Graphene networks with low percolation threshold in ABS nanocomposites: selective localization and electrical and rheological properties, ACS Appl. Mater. Interfaces 6 (2014) 12252–12260, https://doi.org/10.1021/am501843s.
[41] S. Colonna, M.M. Bernal, G. Gavoci, J. Gomez, C. Novara, G. Saracco, A. Fina, Effect of processing conditions on the thermal and electrical conductivity of poly (butylene terephthalate) nanocomposites prepared via ring-opening polymerization, Mater. Des. 119 (2017) 124–132, https://doi.org/10.1016/j.matdes.2017.01.067.
[42] K. Kalaitzidou, H. Fukushima, L.T. Drzal, A new compounding method for exfoliated graphite–polypropylene nanocomposites with enhanced flexural properties and lower percolation threshold, Compos. Sci. Technol. 67 (2007) 2045–2051, https://doi.org/10.1016/j.compscitech.2006.11.014.
[43] A.K. Jonscher, The "universal" dielectric response, Nature 267 (1977) 673–679, https://doi.org/10.1109/57.50801.
[44] D. Wang, X. Zhang, J.-W. Zha, J. Zhao, Z.-M. Dang, G.-H. Hu, Dielectric properties of reduced graphene oxide/polypropylene composites with ultralow percolation threshold, Polymer (Guildf). 54 (2013) 1916–1922.
[45] M.H. Al-Saleh, S. Abdul Jawad, Graphene nanoplatelet–polystyrene nanocomposite: dielectric and charge storage behaviors, J. Electron. Mater. 45 (2016) 3532–3539, https://doi.org/10.1007/s11664-016-4505-6.
[46] M. Trihotri, D. Jain, U.K. Dwivedi, F.H. Khan, M.M. Malik, M.S. Qureshi, Effect of silver coating on electrical properties of sisal fibre-epoxy composites, Polym. Bull. 70 (2013) 3501–3517, https://doi.org/10.1007/s00289-013-1036-7.
[47] M. Trihotri, U.K. Dwivedi, F.H. Khan, M.M. Malik, M.S. Qureshi, Effect of curing on activation energy and dielectric properties of carbon black-epoxy composites at different temperatures, J. Non-Cryst. Solids 421 (2015) 1–13, https://doi.org/10.1016/j.jnoncrysol.2015.04.020.
[48] C. Bessaguet, E. Dantras, C. Lacabanne, M. Chevalier, G. Michon, Piezoelectric and mechanical behavior of NaNbO3/PEKK lead-free nanocomposites, J. Non-Cryst. Solids 459 (2017) 83–87, https://doi.org/10.1016/j.jnoncrysol.2016.12.030.